

# Promoter-free continuous synthesis of high purity single wall carbon nanotube fibers

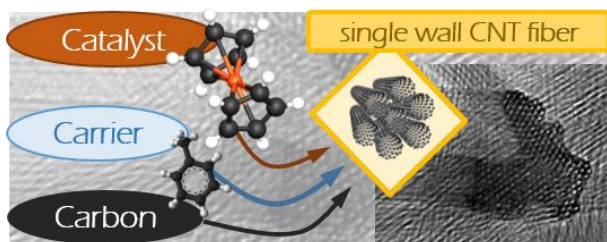
Catharina Paukner\*, Krzysztof K.K. Koziol\*

\* University of Cambridge, Dept Materials Science and Metallurgy  
27 Charles Babbage Road, CB3 0FS Cambridge, UK, cp464@cam.ac.uk

## ABSTRACT

We report a new strategy towards the control of carbon nanotube (CNT) structure and continuous fiber formation using a floating catalyst direct spinning CVD process. In the procedures used to date, a sulphur promoter precursor is added to significantly enhance the rate of CNT formation in the floating catalyst synthesis. Within the reaction zone, the rapidly grown nanotubes self-assemble into bundles, followed by their continuous spinning into fibers, yarns, films or tapes. In this paper we demonstrate a catalyst control strategy in the floating catalyst system, where the CNT formation process is independent of the presence of a promoter but leads to successful spinning of the macroscopic carbon nanotube assemblies with specific morphology, high purity (Raman D/G 0.03) and very narrow diameter range (0.8-2.5 nm). This can be achieved by the control of catalyst precursor decomposition and subsequent formation of homogeneous nanosized catalyst particles.

**Keywords:** single wall carbon nanotubes, floating catalyst CVD, catalyst-free, Raman, TEM



## 1 INTRODUCTION

The particular interest in single wall carbon nanotubes (SWNTs) arises from their remarkable electrical and electronic properties, combining either metallic or semiconducting behaviour (with tunable band gap), very low density and high mechanical performance. Direct spinning of CNT fiber relies on various important parameters which ensures uninterrupted synthesis [1,2]. In this process, the reaction time for nanotube generation takes approximately 3 seconds. The complexity of the process and rapid synthesis can lead to instabilities and formation of undesirable carbonaceous and metallic impurities, interfering with the realisation of macroscopic materials with the outstanding properties of individual CNTs.

Since the early times of direct CVD CNT fiber spinning from various carbon sources (including ethanol and methane) as well as ferrocene (iron catalyst source), a sulphur compound was always required to activate the iron catalyst particles [1]. Sulphur is known to form stable bonds with iron, thereby demobilizing the catalyst on the surface and preserving the particle in its current size, guaranteeing a narrow size distribution of the iron nanoparticles. Iron atoms become available from their ferrocene precursor from about 400 °C [2] and start to collide in the reactor tube. Until carbon becomes available for reaction, the growth of iron particles by coalescence of the atoms is uncontrolled and produces a variety of sizes in iron clusters. Due to its high stability, CH<sub>4</sub> (methane) has a comparatively high pyrolysis temperature and thus carbon only becomes available for reaction with the transition metal at around 1200 °C [2]. In order to keep these clusters small and in a narrow size range, sulphur compounds such as thiophene, carbon disulphide and others have been applied [5-7]. These are less stable and were chosen to release sulphur at temperatures similar to ferrocene pyrolysis [2]. However, too much sulphur present for the reaction entirely encapsulates iron and thus hinders its catalytic activity completely, which leads to soot formation and impurities, which in turn create holes and weak spots in the fiber. As a result, very short, unaligned tubes are formed around the catalyst particles. The presence of short and poorly formed nanotubes generally causes higher defect induced peaks in the Raman spectra. Moreover, S compounds suitable for the spinning process generally show a high toxicity for humans, including impairing fertility. Therefore, developing a process without any S utilization is highly desirable.

Results of the present study show that CNT fiber spinning can be performed successfully without sulphur precursors avoiding the aforementioned drawbacks. To the knowledge of the authors, this paper is the first to report that SWCNT fiber spinning is also possible without sulphur as a promoter, in fact without addition of any sort of heteroatom additive, like sulphur, nitrogen or oxygen. The aim of the study is to show the effects of avoiding sulphur on the morphology of the CNT fibers using a precursor system of toluene and ferrocene. Beside the fact that this process provides a less toxic way to form CNT fibers from fewer ingredients than those reported so far [1,7], the resulting material shows to be cleaner and at optimised conditions made from long bundles of SWCNTs. For details on the experimental setup please refer to [3].

## 2 DISCUSSION

**Sulphur effect.** From findings in the first set of experiments with altered sulphur content in the feedstock (Figure 1), its excessive levels in the synthesis zone have a negative effect on the resulting material. The increased D peak in the respective Raman spectra shows clear evidence for an increase in impurities and defects with thiophene in the feedstock. Similarly the lowering of the 2D peak indicates distortions resulting in a lack of resonance within the CNT graphitic lattice. A possible explanation for this is that sulphur forms a coating on the iron particles [10]. This hinders carbon diffusion into the inner parts of the metal which makes it faster available for incorporation into the forming honeycomb structure which is supported by the observation of slightly lower spinning rates as thiophene is removed from the injection system going down from 60 m/min to 40 m/min. In the case of overinjection however this coating poisons the iron particles, making them unavailable for catalysis. They stay in the sample as impurities, creating defective islands of metal in the CNT bundle network which in turn also induces a decrease in alignment of the bundles within the fiber. Therefore cleaner fiber results as no sulphur is present in the feedstock. In agreement with previous reports a thiophene/toluene ratio in the feedstock of around 0.25 produces collapsed double wall tubes, providing an explanation for the good D-G peak separation as well as the missing RBMs in the Raman spectra [10]. The impressive increase in G peak intensity combined with a clear separation of G' for the sample spun without additive, indicates a distinctly different material from the other samples [11].

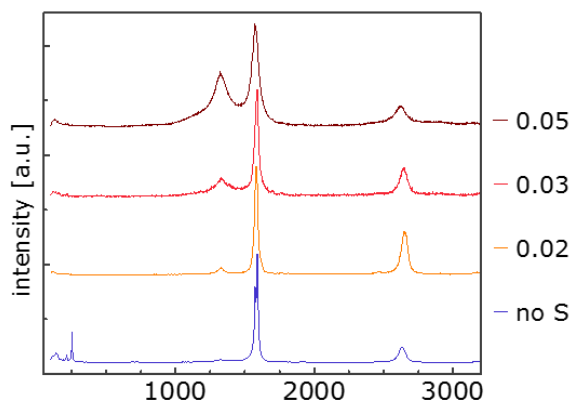


Figure 1: Raman spectra of CNT fiber generated from toluene and ferrocene with (S/C ratio shown in the legend) and without thiophene normalised to the G peak (G=1), offset along the y axis.

**Injection temperature.** It is crucial to note that the heteroatomic additive is not the only potential source of impurities. Floating catalyst CVD is in general a very sensitive method for growing CNTs and will only yield in continuous fiber spinning under very specific ratios of carbon, catalyst and carrier gas. Pyrolysis of toluene at lower

temperatures matches catalyst availability from ferrocene breakdown well and enables CNT formation at an early stage within the reactor. The resulting longer reaction time enables SWCNTs to grow to a length which enables them to bundle up due to van der Waals forces and be extracted as a continuous fiber. Once these feedstock combinations are identified, the morphology of collected samples therefore depends on subtle parameters within the setup. We have been able to identify the injection temperature as one of the most crucial parameters. Apart from the injection depth, this temperature strongly depends on the amount of hydrogen, as well as amount and temperature of the carrier gas stream (helium). The most likely explanation for its significance is its effect on the catalyst precursor. Temperatures higher or close to its pyrolysis point (400 °C) within the injector tube start its decomposition already within that confined space of about 4 mm diameter. The shorter mean free path of the evolving iron nanoclusters<sup>4</sup> causes a higher collision and thus coalescence probability. Resulting bigger catalyst particles are believed to generate CNTs with bigger diameters [12]. Agglomerations of these clusters are not catalytically active for CNT growth and build impurities leading to the observed lower G peak intensity and higher D peak (Figure 2). Similarly they lower the resonance of CNT bundles resulting in lower 2D peak intensities.

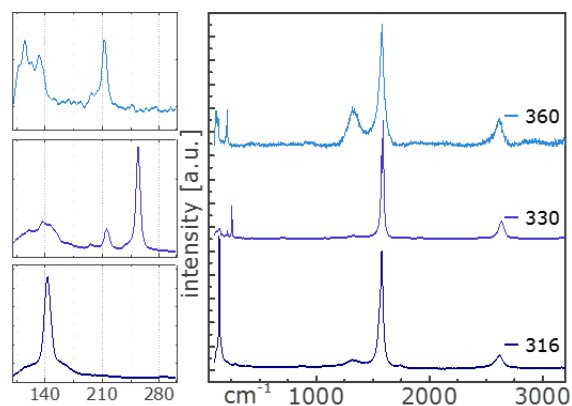


Figure 2: Raman spectra of CNT fiber samples from 15 cm injection depth normalised to the G peak (G=1) listed according to their injection temperature (in °C) with zoom in on RBM region.

Injection at temperatures well below the pyrolysis of ferrocene should in turn result in smaller catalyst particles and CNTs. However we expect that upon lowering the injection temperature further too high dilution of iron within the reactor gives way to catalyst poisoning by excess carbon and again impurities in the fiber. That injection at 5 cm did not yield any CNT fiber may be a result from a too low injection temperature (below 200 °C). It could also be attributed to a convection phenomenon described for the vertical reactor setup [2] probably preventing most of the precursor from advecting into the reaction zone.

The injection temperature affects the morphology of the material obtained from 10 and 15 cm injection depth (Figure

3). Screening samples across the range from 360 (close to ferrocene pyrolysis) to 220 °C, we were able to identify the “turning point”, the injection temperature region optimal for small diameter CNT growth with low defects as  $310 \pm 15$  °C.

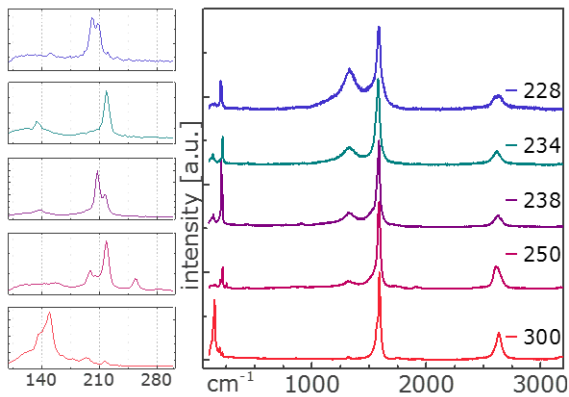


Figure 3: Raman spectra normalised to G for 10 cm injection depth listed according to their injection temperature with a zoom-in on each RBM region.

HRTEM investigations reveal varying tube diameters from 3 to approximately 18 nm for a sample from 15 cm injection depth (15\_1). The random size distribution suggests little control over the catalyst particle size which can be explained by the high temperature at the point of injection (360 °C). Considering that this temperature is close to the pyrolysis temperature of ferrocene (400 °C in hydrogen, Figure 4), it is likely that iron becomes available from the precursor partly already within the injector tube. The shorter mean free path will cause more frequent collision between and thus coalescence of iron atoms to subsequently big but randomly size distributed clusters. Another part of ferrocene will still break up only within the reactor tube, providing an explanation for smaller tubes found in the sample.

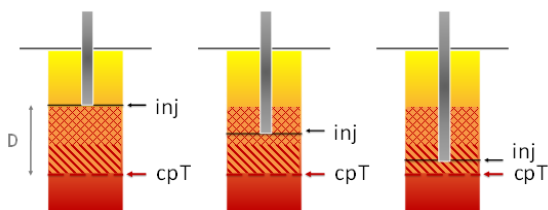


Figure 4: Cat pyrolysis temperature (cpT - at 400 °C) with respect to the injection temperature with distance D.

It is known that CNTs burn in air between 500-800 °C depending on their diameter, number of walls and amount of defects whereby small tubes burn at lower temperatures [13]. Apart from different CNT types, polymeric type substances like carbohydrates could be identified by their lower combustion temperatures between 300-425 °C. A single sharp weight loss thus indicates the presence of CNTs only

with similar diameters without any further carbonaceous impurities which is the case in our samples with iron contents below 3 % (15\_1). To explain this correlation in more detail, it is crucial to understand that the iron remainder in a sample almost never derives from the catalytically active iron particles. High iron residues therefore stem from poisoned – ie carbon coated - clusters of small metal particles. This carbon coating can be of graphitic nature, but always requires defects in the hexagon structure to mimic the shape of the almost spherical or oval metal particles. It will therefore be less stable than carbon nanotubes and show as lower temperature impurities.

The injection temperature in the case of sample 10\_2 was 228 °C which is far below the ferrocene pyrolysis temperature. We should expect a long mean free path for iron atoms within the carrier gas stream. Iron clusters will be comparatively small, but potentially also too small to catalyse the reaction to CNTs. These particles will get poisoned by the carbon as it becomes available and should be visible as impurities in the sample. Randomly distributed bigger clusters of metal should enable the formation of a range of CNTs with potentially wide diameters. Moreover, confirming our assumption in terms of injection temperature, many catalyst particles with various shapes like obelisk, round as well as oval and around them many short tubes can be seen. Together with partly collapsed tubes these provide an explanation for the fairly high D peak in the collected Raman spectra (D/G 0.52). Occasional single wall tubes result in observed RBM peaks (Figure 3). Tube sizes vary evenly between 2 and 16 nm, offering an explanation for the different pyrolysis behaviour found in the TGA spectrum.

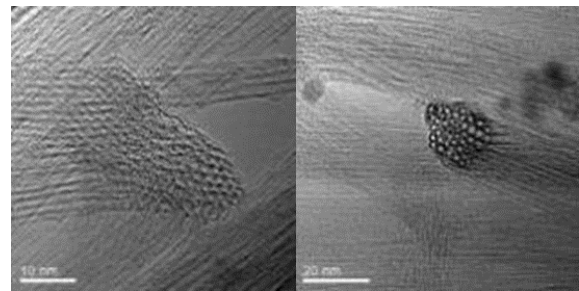


Figure 5: HRTEM of sample 10\_3; SWNT bundle bend and end of a SWNT bundle in top view.

Combination of comprehensive characterisation of samples shows a good agreement between nanostructure investigations in Raman and TEM, as well as microstructure characterisation in SEM and TGA for sample 10\_3, representative for the injection temperature region around 300 °C. SEM revealed a number of surface impurities which are believed to be responsible for the various different low-burning substances identified in TGA. It is proposed that this represents the ideal temperature in terms of ferrocene pyrolysis occurring just after injection but not yet within the injector. Iron particles with a narrow particle size distribution could grow to just the right size for being cata-

lytically active but not further yet by the time carbon becomes available from toluene pyrolysis. Supporting this consideration, TEM images show a number of catalyst particles having almost the same diameter. Moreover, the extremely low disorder found in Raman spectroscopy (D/G 0.03) is supported by TEM images that show barely any impurities apart from superfluous metal particles potentially disturbing the structures in the CNT network (Figure 5). The CNT diameter distribution in this sample is narrow between 0.8 and 2.5 nm. Most counts lie between 1 and 1.5 nm in good agreement measured RBM peaks at 150.0 (1.67), 194.1 (1.27) and 217.1  $\text{cm}^{-1}$  (1.13 nm) (Figure 3).

### 3 CONCLUSIONS

Figure 4 shows pyrolysis of ferrocene (cpT) in relation to the temperature at injection point. At cpT transition metal 400 °C iron atoms become available and will start to collide and coalesce into catalytically active clusters. As the distance D between injection and the point of catalyst precursor pyrolysis gets smaller the collision probability between nascent catalyst atoms is higher and the preceding dispersion period of precursor molecules shorter. A higher number of collisions leads to bigger metal clusters. CNTs display diameters that match these metal cluster sizes. As demonstrated above we found that the injection ideally occurs at about  $310 \pm 15$  °C which leads to mainly SWNTs building up the fiber (Figure 2, sample 316°C and sample 10\_3 Figure 5). At significantly lower injection temperatures (< 230 °C) the longer reaction zone yields a wider variety of tube diameters with on average significantly bigger multi wall tubes (Figure 6, CNT diameter). The greater reactant diffusion also supports formation of by products as demonstrated in Figure 6, Raman D/G vs. injection temperature. Similarly, bigger diameter CNTs are formed as the injection temperature exceeds its optimal range. The proximity of injection to catalyst pyrolysis temperature leads to a partial break up of catalyst already within the injector pipe. The significantly shorter mean free path within the confinement of the injector stem leads to bigger catalyst clusters. The wide CNT diameter range is explainable by some ferrocene pyrolysis within the injector while some of the material does not break up until the bigger volume of the reaction tube.

In this study we show that it was possible to spin SWCNT fiber using a continuous floating catalyst CVD process from ferrocene and a carbon source only, without addition of sulphur or any other heteroatomic precursor. The appropriate carbon source for this experimental setup was found to be toluene. The absence of sulphur in the process enhances the purity of the sample. Indicated by very low D/G ratios in Raman spectra of just 0.03, it was possible to spin CNT fiber with almost no impurities such as polymeric structures or encapsulated iron particles. The catalyst structure is

correlated with the CNT type formed and could be controlled solely by selecting the appropriate carbon source and adjusting the temperature at the injection point.

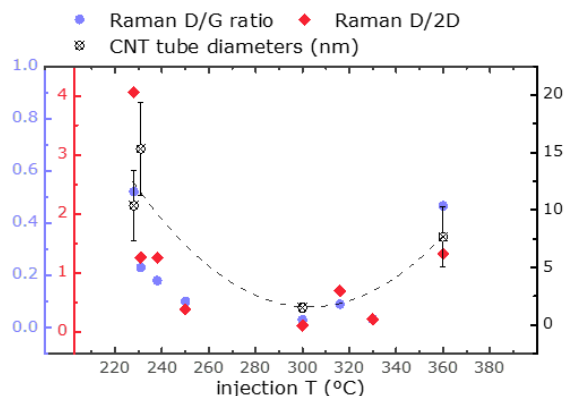


Figure 6: Correlation of D/G (blue circles) and D/2D (red squares) ratios from Raman spectroscopy and the obtained CNT diameter (black hollow circles) with injection temperature.

### REFERENCES

- [1] Li, Y.-L.; Kinloch, I. A.; Windle, A. H. *Science* (80) 2004, 304, 276.
- [2] Conroy, D.; Moiala, A.; Cardoso, S.; Windle, A.; Davidson, J. *Chem. Eng. Sci.* 2010, 65, 2965.
- [3] Paukner, C.; Koziol, K. *Sci. Rep.* 2014, 4, 3903.
- [5] Stano, K. L.; Koziol, K.; Pick, M.; Motta, M. S.; Moiala, A.; Vilatela, J. J.; Frasier, S.; Windle, A. H. *Int. J. Mater. Form.* 2008, 1, 59.
- [6] Koziol, K. K. K.; Ducati, C.; Windle, A. H. *Chem. Mater.* 2010, 22, 4904.
- [7] Sundaram, R. M.; Koziol, K. K. K.; Windle, A. H. *Adv. Mater.* 2011, 23, 1.
- [8] Motta, M.; Kinloch, I.; Moiala, A.; Premnath, V.; Pick, M.; Windle, A. *Phys. E Low-dimensional Syst. Nanostructures* 2007, 37, 40.
- [9] Motta, M. S.; Moiala, A.; Kinloch, I. A.; Windle, A. H. *J. Nanosci. Nanotechnol.* 2008, 8, 2442.
- [10] Jorio, A.; Pimenta, M. A.; Filho, A. G. S.; Saito, R.; Dresselhaus, G.; Dresselhaus, M. S. *New J. Phys.* 2003, 5, 139.1.
- [11] Fiawoo, M.-F.; Bonnot, a.-M.; Amara, H.; Bichara, C.; Thibault-Pénisson, J.; Loiseau, a. *Phys. Rev. Lett.* 2012, 108, 1.
- [12] Schäffel, F.; Kramberger, C.; Ru, M. H.; Grimm, D.; Mohn, E.; Gemming, T.; Pichler, T.; Rellinghaus, B. *Chem. Mater.* 2007, 5006.
- [13] Bom, D.; Andrews, R.; Jacques, D.; Anthony, J.; Chen, B.; Meier, M. S.; Selegue, J. P. *Nano Lett.* 2002, 2, 615.